




Estimation and mapping of Arias intensity in Nepal: Insights from seismic analysis in the Kathmandu Valley

Dibyashree POUDYAL^{1,*} , Norhaiza NORDIN¹ ,
Siti Nur Aliaa ROSLAN² 

¹ Department of Civil Engineering, Infrastructure University Kuala Lumpur, De Centrum City, Jalan Ikram-Uniten, 43000 Kajang, Selangor, Malaysia; e-mails: 082101900007@s.iukl.edu.my; norhaiza.nordin@iukl.edu.my

² Department of Civil Engineering, Universiti Putra Malaysia, 43400 Serdang, Selangor, Malaysia; e-mail: aliaaroslan@gmail.com

Abstract: Kathmandu Valley, the capital of Nepal, is located in the seismically active Himalayan belt and has a history of devastating earthquakes causing substantial loss of life and property damage. This study employs Probabilistic Seismic Hazard Analysis (PSHA) using the Foulser-Piggott Attenuation (FPA) model and *Travasariou et al. (2003)* with R-CRISIS software to calculate Arias intensity in Kathmandu Valley. Historical and recent seismic data within a 500-km radius were analysed, and the earthquake catalogue was declustered and standardized using ZMAP software, a tool developed for the statistical analysis and visualization of earthquake catalogues. Additionally, a Digital Elevation Model (DEM) based topographic analysis was conducted to assess the impact of local topography on seismic site response providing insights into, slope, soil amplification factors, and shear wave velocity across the region. The results reveal Arias intensity values ranging from 0.225 to 0.241 m/s at 2% and 10% probability of exceedance corresponding to 475 and 2475 years, mapped using ArcGIS. The analysis revealed that southwestern Kathmandu and Lalitpur exhibit higher Arias intensity values, while intensity decreases gradually from southwest to northeast. The DEM analysis further revealed that areas with low slopes, particularly in central Kathmandu, have higher soil amplification factors, potentially amplifying seismic waves. The shear wave velocity distribution highlights lower values in sedimentary deposits, indicating increased seismic vulnerability. These findings emphasize the need for effective urban planning and disaster preparedness strategies to mitigate earthquake impacts in Kathmandu Valley.

Key words: Arias intensity, PSHA, shear wave velocity, soil amplification, topographic slope

*corresponding author, e-mail: 082101900007@s.iukl.edu.my

1. Introduction

Arias intensity (I_a) is a seismic parameter that includes seismic amplitude, frequency components, and duration, which may predict certain earthquake damage more reliably than relying solely on seismic amplitude. It can effectively capture the potential damage of earthquakes (*Li et al., 2022*). Arias intensity reflects the energy characteristics of seismic signals over a wide frequency band, that is, the influence of seismic motion throughout its duration. This feature of Arias intensity allows its application in predicting the damage to structures caused by earthquakes (*Sotiriadis et al., 2022*). Kathmandu Valley, which consists of three districts – Kathmandu, Lalitpur, and Bhaktapur is situated in a dynamic tectonic zone, and faces high seismic vulnerability due to the collision of the Indian and Eurasian tectonic plates. This interaction forms the Himalayan mountain range and generates significant seismic activity along major thrusts such as the Main Frontal Thrust (MFT), Main Boundary Thrust (MBT), and Main Central Thrust (MCT) (Fig. 1).

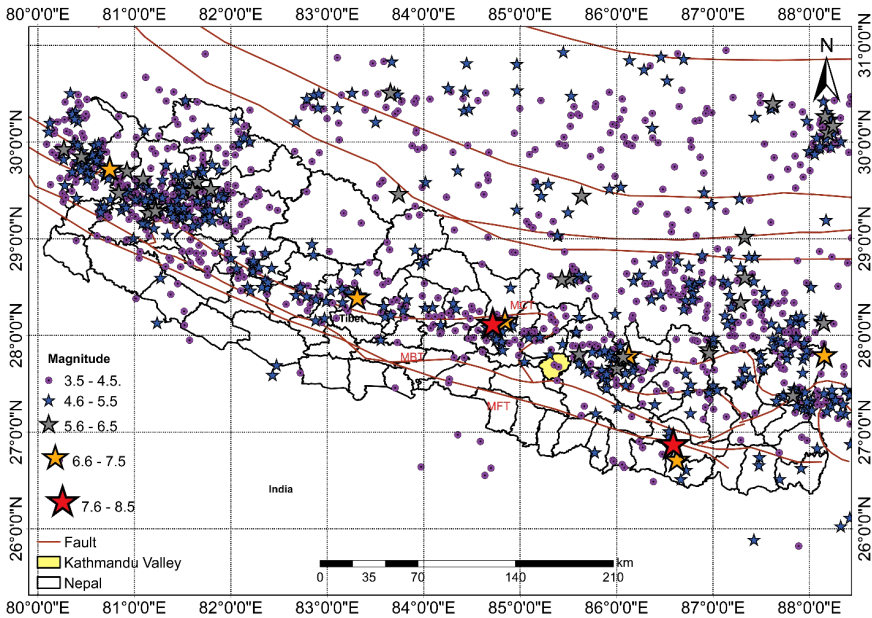


Fig. 1. Major seismic sources of Nepal: MCT, MFT, and MBT with the geographical location of Kathmandu Valley.

The Main Himalayan Thrust (MHT), underlying these structures, has a track record of triggering catastrophic earthquakes. Notable events include the 1934 Nepal-Bihar Earthquake and the 2015 Gorkha Earthquake, both of which caused widespread destruction and loss of life, underscoring the urgent need for effective seismic hazard assessment (*Rajendran, 2021; Pan et al., 2021*). The Kathmandu Valley stands out as a region of critical importance due to its unique vulnerabilities. This region is characterized by high population density, making it highly vulnerable to seismic events due to the sheer number of people and structures at risk. Additionally, the Valley has a large number of historically significant and heritage structures, many of which are centuries old and constructed without modern earthquake-resistant techniques. This makes the region uniquely susceptible to structural damage during earthquakes. Furthermore, past seismic events, including the devastating 1934 Nepal-Bihar Earthquake and the 2015 Gorkha Earthquake, have demonstrated the heightened vulnerability of the Valley due to its soft alluvial soil, which amplifies seismic waves. This combination of factors dense population, fragile construction practices, and historical seismic activity underscores the importance of studying the Kathmandu Valley as a representative and high-risk area for seismic hazard analysis in Nepal (*Poudyal et al., 2024*).

Several studies have developed empirical attenuation relationships for I_a across different tectonic settings. For example, *Tselentis (2011)* developed a non-parametric prediction model using artificial neural networks (ANN) to directly assess the Arias intensity I_a for historic earthquakes, demonstrating that ANN effectively predict I_a from Modified Mercalli Intensity data despite the nonlinear nature of the problem. Similarly, *Lee et al. (2012)* established an empirical I_a attenuation relationship for shallow crustal earthquakes, incorporating fault type and shear wave velocity (V_{S30}) based on Taiwan Strong Motion data, revealing that including V_{S30} reduces regression error and enhances suitability for probabilistic seismic hazard analysis (PSHA). Meanwhile, *Foulser-Piggott and Goda (2014)* developed ground motion models for I_a and Cumulative Absolute Velocity (CAV) using seismic data from Japan, incorporating the 2011 Tohoku event, employing nonlinear random-effects regression analysis to determine model coefficients and evaluate spatial correlation models empirically. In contrast *Rana and Babu (2020)* focused on developing an attenuation relationship

for Arias intensity in the Northeastern region of India, demonstrating the efficacy of the developed equation compared to previous models. Additionally, *Bahrampouri et al. (2021)* developed the equations of Arias intensity for shallow crustal and subduction zone earthquakes in Japan, utilizing the Kiban Kyoshin network database, and incorporating V_{S30} for site effect prediction and additional attenuation for volcanic fronts, applicable for moment magnitudes of 4 to 9. *Sotiriadis et al. (2022)* evaluate the engineering significance of strong-motion parameters like I_a , CAV, and significant duration using the latest strong motion database for Greece, assessing regional and global Ground Motion Models and presenting preliminary PSHA results for selected sites, investigating the feasibility of using Arias intensity I_a as an alternative threshold parameter for PSHA instead of CAV. Meanwhile, *(Xu et al., 2023)* developed a new seismic source model for mainland China, employing PSHA to estimate earthquake probabilities from 2021 to 2030 and determine the hazard by choosing suitable ground motion for China seismic source.

Few studies have previously undertaken PSHA for Nepal including Kathmandu Valley to calculate the peak ground acceleration (PGA) at the bedrock level with varying probabilities of exceedance but without incorporating topographic effects. Previous studies by *Parajuli et al. (2010)* and *Thapa and Wang (2013)*, employ a probabilistic approach to estimate seismic ground motion hazard in Nepal, to calculate the PGA at the bedrock level with varying probabilities of exceedance. Likewise, *Rahman and Bai (2018)* utilize three seismogenic source models to conduct PSHA in Nepal, incorporating long-term slip rates and paleoseismic records, revealing significant spatial variability in seismic hazard levels highlighting the high potential in the Lesser Himalaya and along the MHT. While *Pokhrel et al. (2019)* performed a PSHA for the Kathmandu basin, highlighting the requirement of a tailored ground motion model for Nepal whereas *Pradhan et al. (2020)* use R-CRISIS 2007 software to carry out the PSHA of Nepal to generate a PGA map at bedrock level for Nepal. As the capital and most densely populated region (2.9 million) in the country, the Kathmandu Valley is a focal point for seismic risk assessment because it houses critical infrastructure, cultural heritage sites, and a large population living in structures that may not comply with modern earthquake-resistant standards (*Poudyal et al., 2024*). Arias intensity (I_a) offers several advantages over traditional pa-

rameters like Peak Ground Acceleration (PGA) and Peak Ground Velocity (PGV), making it a superior metric for seismic risk assessment. Unlike PGA and PGV, which primarily measure instantaneous peak ground motion, I_a provides an energy-based measure of seismic shaking that accounts for the entire duration of an earthquake. This is particularly valuable in regions like the Kathmandu Valley, where the geological structure and soft alluvial deposits amplify seismic waves, resulting in prolonged shaking. Additionally, I_a captures the full frequency spectrum of seismic motion, reflecting the energy characteristics of an earthquake more comprehensively than PGA or PGV, which focus on limited frequency bands. Furthermore, I_a is more sensitive to site-specific effects, such as basin amplification, and aligns well with advanced probabilistic seismic hazard analysis (PSHA) models, reducing bias in predictive modelling. These attributes make I_a particularly suitable for assessing seismic risk in the Valley, where high population density, fragile infrastructure, and ancient structures demand a comprehensive metric for disaster preparedness and resilience planning.

Additionally, none of the studies calculates the topographical slope to determine the soil amplification and shear wave velocity of Kathmandu Valley. Traditional methods for estimating soil amplification and shear wave velocity (V_{S30}) often rely on direct geophysical or geotechnical investigations, such as borehole measurements, seismic refraction, and surface wave analysis. While this method provides accurate localized data, they are costly, time-consuming, and impractical for large-scale applications, particularly in regions with limited field data availability. In contrast, using topographic slope as a proxy for seismic site characterization offers a more efficient and scalable approach, as it leverages readily available Digital Elevation Models (DEMs).

2. Data and methodology

2.1. Preparation of earthquake catalogue

Identifying seismic sources is the initial stage in PSHA which necessitates the collection of past seismic data and updating a seismic database. For this study, 4324 events from the year 2000 to 2023 AD with magnitudes ranging from 3.5 to 8.5 shown in Fig. 1 were compiled by amalgamating data from different sources, including US Geological Survey the International

Seismological Centre, and the Integrated Research Institutes for Seismology. However, the catalogue used in this study was heterogeneous, as it contained data from different agencies and literature sources, represented in different magnitude measures.

To standardize the catalogues, all the magnitudes were converted into M_w the moment magnitude scale. M_w was chosen due to the limitations of other scales like surface wave magnitude (M_s), body wave magnitude (M_b), and local magnitude (M_l) which is applicable over specific distance and frequency interval. M_w provides the precise estimation for significant earthquakes, but converting other scales to M_w requires empirical correlations specific to each region. Conversion of M_s , M_b and M_l to M_w were employed by the relationships formulated by *Wason et al. (2012)*, *Das et al. (2012)*, and *Ristau et al. (2005)*, respectively. Additionally, moment magnitude provided by *Das et al. (2012)* was calculated from seismic data using intensity measures by utilizing an empirical connection (1), where, MMI is Modified Mercalli Intensity:

$$M_w = 0.762 \text{ MMI} + 0.865. \quad (1)$$

The seismic event catalogue was compiled with the aforementioned relations. This database initially contained redundant seismic records, indicating multiple recordings of the same event. To address this, a preliminary elimination step was conducted to remove duplicate occurrences prioritizing the accuracy and reliability of the data sources. The catalogue consisted of various types of events, including aftershocks, foreshocks, and mainshocks, all resulting from seismic and residual stress changes originating from the main event. To obtain an independent dataset, these dependent events are eliminated by declustering.

In this study, the Gardner and Knopoff algorithm was employed for declustering, using ZMAP software. The range and duration of the aftershock sequence were determined relative to the mainshock. Following declustering, it became apparent that the catalogue lacked completeness across different periods and magnitude ranges. Higher magnitude events exhibited more consistent records compared to lower magnitude occurrences, underscoring the importance of catalogue completeness in capturing seismicity patterns accurately. Stepp's method was assessed to evaluate the completeness of the earthquake catalogue (*Stepp et al., 2001*).

2.2. Delineation of seismic source zone

Kathmandu Valley faces seismic hazards arising from both close and far-off seismic events. The seismic source zones identified in this study primarily impact the Valley but also extend to certain areas in north India, west Bhutan, and south Tibet. The assessment of seismic risk in a particular area starts with the identification of seismic source areas. Owing to limited information on individual faults the analysis focused on areal sources for seismic modelling. The study area was divided into 24 distinct source zones as illustrated in Fig. 2 each considered to be seismically uniform, implying that any point within a zone has an equal likelihood of experiencing an earthquake in the future using a pattern recognition approach outlined by *Gelfand et al. (1972)*. These 24 zones vary in size and seismic hazard characteristics. The hazard parameters utilized in this study are detailed in the subsequent sections. A high concentration of earthquakes was noted in the far western region (Z15 to Z16) of Nepal indicating high tectonic activity. The eastern region of Nepal (zones Z10 to Z11 and Z22 to Z24) also exhibits high seismicity clusters. The easternmost zone (seismic source

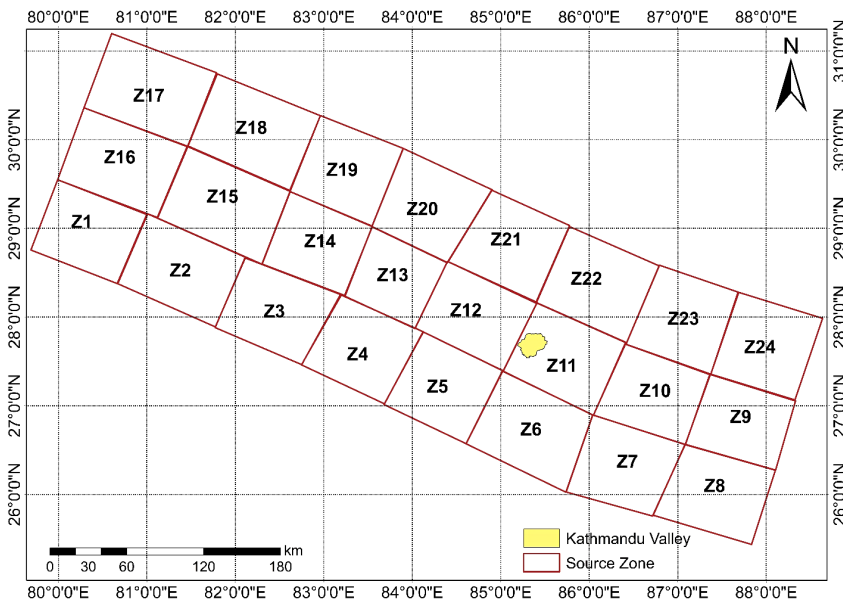


Fig. 2. Delineated seismic source zones in and around the Kathmandu Valley.

zone Z24) encompasses parts of north India, the western region of Bhutan, eastern Nepal, and southern Tibet. Source zones Z10, Z12, and Z13, in the past have produced at least one significant earthquake. The seismic zone Z12 has a record of two strong earthquakes in the past. No records of strong earthquakes were found in the seismic zones Z5 and Z19.

2.3. Determination of recurrence parameters

Using Gutenberg-Richter’s recurrence law, recurrence parameters a and b which follow the Poisson distribution are derived. According to this law, earthquakes happen independently of each other in both time and location. The mathematical representation of average rate exceedance (λ_m) of magnitude m given by Gutenberg-Richter law can be expressed as:

$$\log \lambda_m = a - bm. \tag{2}$$

ZMAP software was used to ascertain these values, along with the magnitude of completeness (M_c). The Kijko-Sellevol-Bayes approach is used to calculate the maximum magnitude.

2.4. Ground motion prediction models

These seismic models serve the purpose of assessing the response spectrum and depicting the attenuation characteristics of a particular area. In this study, FPA model known as Foulser-Piggott Attenuation model and *Travasari et al. (2003)* is employed to generate maps for Arias intensity (I_a). Several empirical correlations have been established to associate earthquake-induced ground motions with I_a . I_a acts as a measurable indicator of the intensity of shaking generated by seismic activity. It is the total energy absorbed per unit mass by a set of simple undamped oscillators, with zero to infinity as their resonance frequencies (*Mercurio et al., 2023*):

$$I_a = \frac{\pi}{2g} \int_0^{T_d} a(t)^2 dt. \tag{3}$$

The analysis incorporates factors such as the documented acceleration time-history $a(t)$, acceleration due to gravity (g), along with the duration of ground motion (T_d). *Wilson and Keefer (1985)* pioneered the development of the Arias intensity, and attenuation relationship which connected the occurrence of earthquake triggered landslides with this strength metric. The

dataset comprises the eight earthquakes recorded in California, Japan, and Hawaii, using regression analysis. Bachman and Machette in 1987 employed the same dataset but supplemented it with data from Tabas earthquake Iran to formulate an alternative equation for computing I_a (Foulser-Piggott and Goda, 2015). Similarly, Travasarou investigated the efficacy of utilizing I_a to assess the earthquake resilience of infrastructure primarily affected by significant ground motion. They developed a nonlinear regression analysis, and the model was robust and adaptable, it has some drawbacks, especially when it comes to simulating shallow-depth site reaction. Consequently, a Foulser-Piggott Attenuation (FPA) model was established. Equation (4) expresses the universally applicable FPA model:

$$\log I_a = c_1 - c_2 * (8.5 - M)^2 + (c_3 - c_4 M) * \ln \left(\sqrt{R^2 + c_5^2} \right) + c_6 * F_{RV}, \quad (4)$$

where, F_{RV} is a variable. The shallow crustal earthquakes for which the FPA model is intended occur at distances of less than 100 km and moment magnitudes ranging from 5 to 8. A weightage of 0.6 was given to the FPA model, created using the most current database, while a weightage of 0.4 was given to the Travasarou model.

2.5. Seismic hazard assessment

PSHA method proposed by Cornell (1968) was used in this study, to assess the seismic hazards. According to this method, the likelihood of surpassing a specified value x of a seismic intensity parameter X , for a potential seismic event at a given source location is computed. This likelihood is subsequently multiplied by the probability of occurrence of an earthquake at that particular site, as represented by Eq. (5):

$$P(X > x) = \int_{m_{\min}}^{m_{\max}} \int_0^{T_{\max}} P(X > x | m, r) f_m(m) f_r(r) dr dm. \quad (5)$$

The PDF probability density functions are represented by variables $f_M(m)$ and $f_R(r)$ respectively, and $P(X > x | m, r)$ is obtained from the model. Therefore, for analysis, distance is split into discrete intervals and magnitude is split into ranges. This process is iterated for magnitudes and all potential locations. Equation (5) can be extended to accommodate multiple sources (N_s), each characterized by mean occurrence rate of ground motion threshold, and the overall exceedance rate is determined by Eq. (6).

$$\lambda(X > x) = \sum_{i=1}^{N_s} \int_{m_{\min}}^{m_{\max}} \int_0^{r_{\max}} P(X > x | m, r) f_m(m) f_r(r) dr dm. \quad (6)$$

However, evaluating the integrals in the equations analytically to predict realistic PSHA outcomes is challenging due to the complexity of the parameters involved. The PSHA is conducted by R-CRISIS software and a suite of MATLAB programs based on Poisson’s model. Every designated zone is given a range of maximum as well as minimum magnitudes together with recurrence parameters, and it was depicted as an area source. These sources were discretized by the software using a triangulation approach, and the procedure was repeated until predetermined requirements were satisfied. The minimum triangle size (S) and the ratio of source-to-site distance to the triangle size (R) were among these requirements. Sensitivity analysis involved assessing various combinations of S and R values. A recursive function allowed each source with “ N ” vertices to be initially subdivided into $N-2$ triangles, and so on until the desired S or R value was reached. The distance from the source to the site was computed, and the distance between the centroid of each triangle represents the seismicity of region source. R-CRISIS employed the integration method to sample seismicity source models taking into account all potential seismic locations within the source. In order to visualize the results of the hazard analysis, hazard maps were generated. The Arias intensity for return periods of 475 years and 2475 years was calculated.

2.6. Computation of topographic slope, soil amplification, and shear wave velocity

The computational approach for estimating topographic slope, soil amplification, and shear wave velocity (V_{S30}) was implemented using MATLAB, in the Kathmandu Valley. The analysis began with processing a Digital Elevation Model (DEM). The DEM dataset contained metadata, including spatial reference information, coordinate limits, and resolution. The study area was then extracted using a bounding box defined in WGS 1984 geographic coordinates. The topographic slope was computed using the gradient method, where elevation changes in the x and y directions (dz/dx , dz/dy) were calculated using the MATLAB gradient function. These gradients were normalized using the DEM spatial resolution, and converted to

meters based on an approximate conversion factor of 111,320 meters per degree. The slope was then computed in degrees using the inverse tangent function. To estimate the soil amplification factor and average shear wave velocity (V_{S30}) the empirical model proposed by *Allen and Wald (2009)* which accounts for topographic effects in seismic hazard assessment based on topographic slope was used.

3. Results

The seismic hazard analysis of Kathmandu Valley was conducted by the PSHA method, and is presented as an Arias intensity map in Fig. 3 at 2% and 10% of the probability of exceedance in 50 years. The seismic hazard map for a 2% probability of exceedance closely resembles that observed for a return period of 475 years. However, for a longer return period, a substantial portion of the area exhibits elevated intensity values, indicating heightened vulnerability to seismic hazards. Due to urbanization and the movement of people from remote areas to the Kathmandu Valley are major concerns of this study. The observed values vary from 0.581 to 0.658 m/s and 0.207 to 0.241 m/s corresponding to 2475 and 475 years respectively. The results highlight significant differences in the seismic energy distribution within the Valley. Central Kathmandu shows moderate Arias intensity

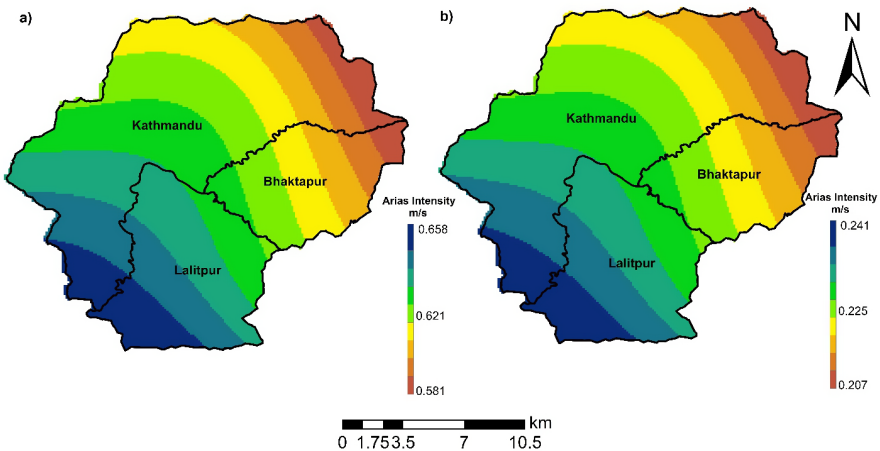


Fig. 3. Arias intensity map at 2% and 10% probability of exceedance for the Valley.

values, with a gradual decrease from southwest to northeast. Southwestern Kathmandu and Lalitpur exhibit the higher Arias intensity values, around 0.225 to 0.241 m/s.

The results of the DEM-based topographic analysis for Kathmandu Valley include three key outputs: topographic slope, soil amplification factor, and shear wave velocity (V_{S30}) as shown in Fig. 4. The soil amplification map shows that areas with low topographic slopes, particularly in the central valley, exhibit higher amplification factors. This observation aligns with *Allen and Wald (2009)*, which suggests that low-slope regions, often consisting of thick, unconsolidated sediments, experience greater seismic wave amplification. The highest amplification values, near 3, are concentrated in sedimentary deposits, while lower values are found in steeper, bedrock-dominated regions. The shear wave velocity distribution shows an inverse relationship with the soil amplification factor. Low V_{S30} values ($\sim 200 - 400$ m/s) are observed in the central valley region.

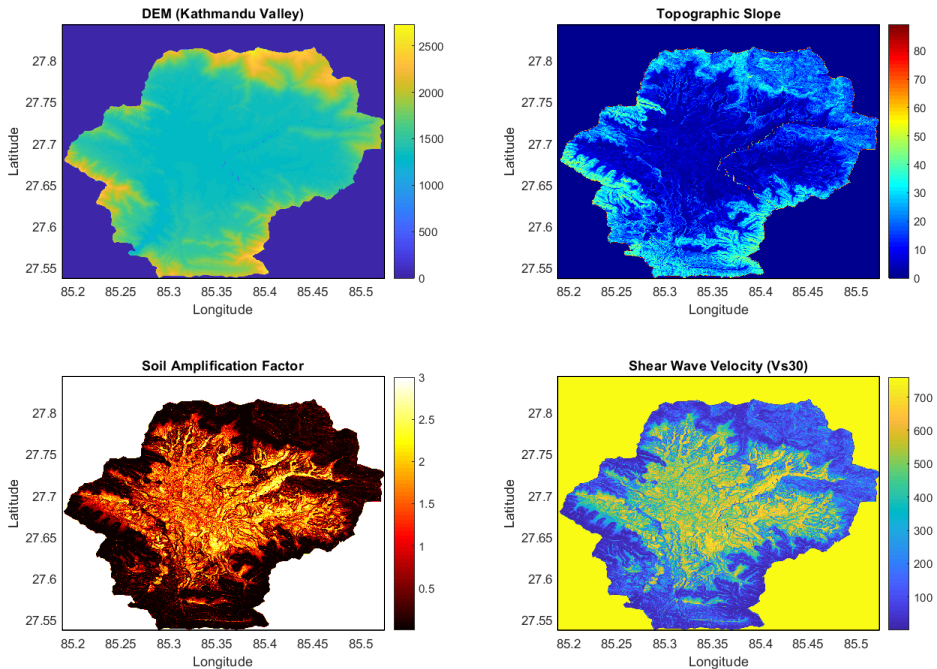


Fig. 4. DEM based topographic analysis of Kathmandu Valley showing DEM model, topographic slope, soil amplification factor, and shear wave velocity.

4. Discussions

The seismic hazard analysis of the Valley using the PSHA method has provided critical insights into the spatial variation of Arias intensity across three districts of the Valley. Historical landmarks, including Durbar Squares in Kathmandu, Bhaktapur, and Patan, experienced severe destruction, highlighting the vulnerability of heritage sites to strong ground shaking. Infrastructure damage, such as subsidence along the Araniko Highway and liquefaction in Kathmandu Valley, further supports the significance of Arias intensity values in assessing seismic risks. The findings from the DEM-based analysis and Arias intensity distribution reveal a strong correlation between local site conditions and seismic response in Kathmandu Valley. The higher Arias intensity values observed in Bhaktapur align with regions exhibiting higher soil amplification and lower V_{S30} values, confirming the influence of soil conditions on seismic shaking. This suggests that softer soils with lower V_{S30} amplify ground motion, leading to increased seismic hazard. The topographic slope also plays a role, as steeper terrains may experience localized amplification due to topographic effects, which is reflected in the spatial distribution of Arias intensity. The validation of DEM-based parameters through Arias intensity underscores the importance of integrating elevation, soil properties, and shear wave velocity in seismic hazard assessment. The strong correlation between soil amplification and Arias intensity highlights that ground motion intensity is significantly influenced by local geological and geomorphological factors. Previous studies reveal that the V_{S30} pattern observed is consistent with the findings of (*Poudyal et al., 2024*), which indicate low V_{S30} values in the Kathmandu basin due to thick sedimentary layers. The high soil amplification factors in central Kathmandu are also in line with site effects observed during the 2015 Gorkha earthquake, where ground shaking was amplified due to soft sediments. However, the *Allen and Wald (2009)* model, while useful for estimating V_{S30} based on topographic slope, may not fully capture local geological variations, and using a reference V_{S30} of 760 m/s for flat terrain may overestimate V_{S30} in soft sediment areas. The findings have important implications for seismic hazard assessment. The low V_{S30} and high soil amplification in central Kathmandu suggest higher seismic vulnerability, underscoring the need for seismic microzonation and structural retrofitting in the region. Future studies should

integrate geotechnical data and site-specific V_{S30} measurements to further refine seismic hazard models for Kathmandu Valley.

5. Conclusion

The seismic vulnerability of the Kathmandu Valley is significantly influenced by its geological conditions, which amplify ground shaking and result in higher Arias intensity values. The probabilistic seismic hazard analysis conducted for Valley reveals the Arias intensity in the range of 0.207 to 0.241 m/s and 0.581 to 0.658 m/s corresponding to 475 years and 2475 years. These findings highlight the varying levels of seismic risk across different time frames, with significantly higher intensity values associated with the longer return period, indicating a greater potential for severe ground shaking and related damage over extended intervals. The analysis demonstrates that Central Kathmandu shows moderate Arias intensity values, with a gradual decrease from southwest to northeast. Southwestern Kathmandu and Lalitpur exhibit higher Arias intensity values, around 0.225 to 0.241 m/s. DEM based analysis further reinforces these findings by identifying topographic and geophysical factors that influence seismic response. Areas with steep slopes and lower V_{S30} values are associated with higher soil amplification, leading to greater ground motion intensity. The spatial correlation between DEM derived soil amplification and Arias intensity values confirms that local site conditions play a crucial role in seismic hazard. In particular, Bhaktapur and southwestern Kathmandu, where higher soil amplification and lower V_{S30} values were observed, show increased Arias intensity, highlighting the need for site-specific risk mitigation. To mitigate the high seismic intensity and its associated risks in Valley, a multi-faceted approach is necessary, focusing on urban planning, construction practices, and community preparedness. It is essential to implement and strictly enforce updated building codes and standards, ensuring that all new constructions adhere to the latest earthquake-resistant design requirements. Retrofitting existing vulnerable structures, particularly historical buildings and critical facilities, should be prioritized to enhance their resilience against higher Arias intensity values. Furthermore, incorporating DEM-based geospatial analyses in seismic hazard assessments can improve risk modelling and land-use planning, helping to identify and safeguard high-risk zones.

Funding. This research did not receive any specific grant from funding agencies.

Conflict of interest statement. The authors declare that they have no conflicts of interest.

Data availability. The data underlying this article will be shared on reasonable request to the corresponding author.

References

- Allen T. I., Wald D. J., 2009: On the use of high-resolution topographic data as a proxy for seismic site conditions (V_{S30}). *Bull. Seismol. Soc. Am.*, **99**, 2A, 935–943, doi: 10.1785/0120080255.
- Bahrampouri M., Rodriguez-Marek A., Green R. A., 2021: Ground motion prediction equations for Arias Intensity using the Kik-net database. *Earthq. Spectra*, **37**, 1, 428–448, doi: 10.1177/8755293020938815.
- Cornell C. A., 1968: Engineering seismic risk analysis. *Bull. Seismol. Soc. Am.*, **58**, 5, 1583–1606, doi: 10.1785/BSSA0580051583.
- Das R., Wason H. R., Sharma M. L., 2012: Temporal and spatial variations in the magnitude of completeness for homogenized moment magnitude catalogue for northeast India. *J. Earth Syst. Sci.*, **121**, 1, 19–28. doi: 10.1007/s12040-012-0144-3.
- Foulser-Piggott R., Goda K., 2014: New prediction equations of Arias intensity and cumulative absolute velocity for Japanese earthquakes. In: *Proc. 2nd ECEES*, 25–29 August 2014, Istanbul, Turkey, pp. 1277–1287, available at: <http://www.kyoshin.bosai.go.jp/>.
- Foulser-Piggott R., Goda K., 2015: Ground-motion prediction models for arias intensity and cumulative absolute velocity for Japanese earthquakes considering single-station sigma and within-event spatial correlation. *Bull. Seismol. Soc. Am.*, **105**, 4, 1903–1918, doi: 10.1785/0120140316.
- Gelfand I. M., Guberman Sh. I., Izvekova M. L., Keilis-Borok V. I., Ranzman E. Ja., 1972: Criteria of high seismicity, determined by pattern recognition. *Dev. Geotecton.*, **4**, 415–422, doi: 10.1016/B978-0-444-41015-3.50028-8.
- Lee C.-T., Hsieh B.-S., Sung C.-H., Lin P.-S., 2012: Regional Arias intensity attenuation relationship for Taiwan considering V_{S30} . *Bull. Seismol. Soc. Am.*, **102**, 1, 129–142, doi: 10.1785/0120100268.
- Li X., Xu W., Gao M., 2022: Probabilistic Seismic Hazard Analysis Based on Arias Intensity in the North–South Seismic Belt of China. *Bull. Seismol. Soc. Am.*, **112**, 2, 1149–1160, doi: 10.1785/0120210106.
- Mercurio C., Calderón-Cucunuba L. P., Argueta-Platero A. A., Azzara G., Cappadonia C., Martinello C., Rotigliano E., Conoscenti C., 2023: Predicting Earthquake-Induced Landslides by Using a Stochastic Modeling Approach: A Case Study of the 2001 El Salvador Coseismic Landslides. *ISPRS Int. J. Geo-Inf.*, **12**, 4, 178, doi: 10.3390/ijgi12040178.

- Pan Y., Chang Z., Li C., Shi, S., 2021: Ground motion characteristics of the 2015 Gorkha earthquake sequence. *Earthq. Struct.*, **20**, 6, 617–626, doi: 10.12989/eas.2021.20.6.617.
- Parajuli H. R., Kiyono J., Taniguchi H., Toki K., Maskey P. N., 2010: Probabilistic seismic hazard assessment for Nepal. *WIT Trans. Inf. Commun. Technol.*, **43**, 405–416, doi: 10.2495/RISK100351.
- Pokhrel R. M., De Risi R., Werner M. J., De Luca F., Vardanega P. J., Maskey P. N., Sextos A., 2019: Simulation-based PSHA for the Kathmandu Basin in Nepal. In: *Proc. 13th International Conference on Applications of Statistics and Probability in Civil Engineering(ICASP13)*, Seoul, South Korea, May 26-30, 2019, pp. 1–8, doi: 10.22725/ICASP13.344.
- Poudyal D., Nordin N., Roslan S. N. A., Dahalet B. K., 2024: Spatial mapping of seismic vulnerability index in Kathmandu Valley: Insight from dominant frequency and amplification factor. *J. Geophys. Eng.*, **21**, 4, 1272–1285, doi: 10.1093/jge/gxae069.
- Pradhan P. M., Timalisina S. P., Bhatt M. R., 2020: Probabilistic seismic hazard analysis for Nepal. *Lowl. Technol. Int.*, **22**, 1, 75–80, https://cot.unhas.ac.id/journals/index.php/ialt_lti/article/view/803.
- Rahman M. M., Bai L., 2018: Probabilistic seismic hazard assessment of Nepal using multiple seismic source models. *Earth Planet. Phys.*, **2**, 4, 327–341, doi: 10.26464/epp2018030.
- Rajendran C. P., 2021: Constraints on previous earthquakes from the liquefaction sites in the Kathmandu Valley associated with the 2015 Gorkha earthquake and their regional implications. *Quat. Int.*, **585**, 44–54, doi: 10.1016/J.QUAINT.2020.10.053.
- Rana H., Babu G. L. S., 2020: Predictive model for Arias intensity in northeastern region of India. In: *Proc. 16th Asian Regional Conference on Soil Mechanics and Geotechnical Engineering, ARC 2019*, October 14–18, 2019, Taipei, Taiwan, pp. 2–5.
- Ristau J., Rogers G. C., Cassidy J. F., 2005: Moment magnitude–local magnitude calibration for earthquakes in western Canada. *Bull. Seismol. Soc. Am.*, **95**, 5, 1994–2000, doi: 10.1785/0120050028.
- Sotiriadis D., Margaris B. N., Klimis N., Dokas I. M., 2022: Evaluation of Ground Motion Models for Arias Intensity (I_A), Cumulative Absolute Velocity (CAV) and Significant Duration for Greece and Preliminary PSHA results. *Proc. 3rd International Conference on Natural Hazards and Infrastructure*, 5–7 July 2022, Athens, Greece, pp. 1–12.
- Stepp J. C., Wong I., Whitney J., Quittmeyer R., Abrahamson N., Toro, G., Youngs R., Coppersmith K., Savy J., Sullivan T., Yucca Mountain PSHA project members, 2001: Probabilistic seismic hazard analyses for ground motions and fault displacement at Yucca Mountain, Nevada. *Earthq. Spectra*, **17**, 1, 113–151, doi: 10.1193/1.1586169.
- Thapa D. R., Wang G., 2013: Probabilistic seismic hazard analysis in Nepal. *Earthq. Eng. Eng. Vib.*, **12**, 4, 577–586, doi: 10.1007/s11803-013-0191-z.
- Travasarou T., Bray J. D., Abrahamson N. A., 2003: Empirical attenuation relationship for Arias Intensity. *Earthq. Eng. Struct. Dyn.*, **32**, 7, 1133–1155, doi: 10.1002/eqe.270.

- Tselentis G.-A., 2011: Assessment of Arias Intensity of historical earthquakes using modified Mercalli intensities and artificial neural networks. *Nat. Hazards Earth Syst. Sci.*, **11**, 12, 3097–3105, doi: 10.5194/nhess-11-3097-2011.
- Wason H. R., Das R., Sharma M. L., 2012: Magnitude conversion problem using general orthogonal regression. *Geophys. J. Int.*, **190**, 2, pp. 1091–1096, doi: 10.1111/j.1365-246X.2012.05520.x.
- Wilson D. K., Keefer R. C., 1985: Predicting areal limits of earthquake-induced landsliding. In: Ziony J. I. (Ed.): *Evaluating Earthquake Hazards in the Los Angeles Region: An Earth-Science Perspective*. U.S. Geological Survey Professional Paper 1360, pp. 316–345.
- Xu W., Wu J., Gao M., 2023: Seismic Hazard Analysis of China's Mainland Based on a New Seismicity Model. *Int. J. Disaster Risk Sci.*, **14**, 2, 280–297, doi: 10.1007/s13753-023-00487-w.